Marine Geology 489 (2025) 107637

Contents lists available at ScienceDirect

Marine Geology

journal homepage: www.elsevier.com/locate/margo

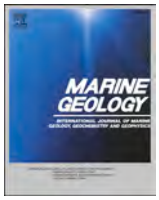

Research Article

A thousand-year journey of lithification: CT-analysis and radiocarbon dating of algal reef from Central Mediterranean

Pietro Bazzicalupo [a,*], Valentina Alice Bracchi [a,b], Mara Cipriani [c], Adriano Guido [c], Antonietta Rosso [d], Rossana Sanfilippo [d], Francesco Maspero [a], Anna Galli [e], Elena de Ponti [f], Daniela Basso [a,b]

[a] Department of Environmental and Earth Sciences, University of Milano-Bicocca, Piazza della Scienza 4, 20126 Milano, Italy
[b] CoNISMa, Piazzale Flaminio 9, I-00196 Roma, Italy
[c] Department of Biology, Ecology and Earth Sciences, University of Calabria, Via P. Bucci, cubo 15b Rende, I-87036 Cosenza, Italy
[d] Department of Biological, Geological and Environmental Sciences, University of Catania, Corso Italia 57, I-95129 Catania, Italy
[e] Department of Material Sciences, University of Milano-Bicocca, Via Roberto Cozzi 55, I-20125 Milano, Italy
[f] Department of Sanitary Physics, ASST Monza, Via G. B. Pergolesi, 33, 20900 Monza, Italy

ARTICLE INFO

Editor: Shu Gao

Keywords:
Coralligenous reefs
CT-Scan
Radiocarbon dating
Mediterranean Sea

ABSTRACT

Calcareous algal reefs are Mediterranean carbonate structures, formed by coralline red algae, that display early lithification and preserve key geobiological records. These structures exhibit complex three-dimensional frameworks influenced by environmental conditions and biological interactions, but their lithification processes, porosity evolution, and long-term growth patterns remain poorly understood. In this study, we use Computed Tomography (CT) scanning and radiocarbon dating on four coralligenous build-ups collected along a depth gradient offshore Marzamemi, SE Sicily, to investigate internal skeletal density, porosity distribution, and age profiles. Our findings reveal that lithification progresses gradually from High-Density (HD) to Ultra-High-Density (UHD) material, correlating inversely with porosity. Radiocarbon dating indicates a lithification timeline of roughly 1000 years, with the oldest, densest material dating back over 5000 years. The structures demonstrate a depth-density and age-depth gradient: deeper and older build-ups exhibited higher quantity of UHD material, whereas younger, shallower build-ups contain a higher proportion of HD material. Additionally, evidence suggests that specific build-ups may have been fragmented and relocated due to environmental or anthropogenic factors, further influencing growth patterns. The CT-analysis contributes to improving knowledge on coralligenous reef formation and evolution, underscoring the role of lithification in maintaining structural stability over millennia and providing insights applicable to the study of fossil reef systems.

1. Introduction

Coralligenous build-ups are highly intricate and specialised marine habitats that are fundamental to the ecological integrity of the Mediterranean Sea. These submerged formations are primarily composed of crustose calcareous red algae (Ballesteros, 2006; Basso et al., 2022) which construct three-dimensional reef-like structures. As such, they serve as essential habitats for a diverse array of marine species and play a central role in the overall health and balance of the Mediterranean environment (e.g., Ferrigno et al., 2023; Piazzi et al., 2022; Piazzi et al., 2012).

The morphological diversity of coralligenous reefs, ranging from vertical banks to massive plateau and discrete structures (Bracchi et al., 2017), distributed in the 20–140 m bathymetric range is closely associated with environmental variables (Laborel, 1961, 1987). The main coralligenous algal framework forms biogenic structures from a few centimetres to several metres thick (Pérès, 1982; Laborel, 1987; Bracchi et al., 2017; Basso et al., 2022). In addition to coralline algae, other critical constructors include bryozoans, serpulid polychaetes, cnidarians and mollusks (Ballesteros, 2006; Rosso and Sanfilippo, 2009; Corriero et al., 2019; Cardone et al., 2022; Rosso et al., 2023; Donato et al., 2024 Sanfilippo et al., 2024). Furthermore, the high porosity of the internal framework provides diverse cavities and microcavities suitable for the life of cryptic metazoan and microbial communities whose metabolic

* Corresponding author at: Department of Environmental and Earth Sciences, University of Milano-Bicocca, Piazza della Scienza 4, 20126 Milano, Italy.
E-mail address: pietro.bazzicalupo@unimib.it (P. Bazzicalupo).

https://doi.org/10.1016/j.margeo.2025.107637
Received 17 December 2024; Received in revised form 19 July 2025; Accepted 15 August 2025
Available online 21 August 2025

activity and taphonomy-related processes induce autochthonous micrite precipitation. This phenomenon contributes to strengthening the coralligenous structures due to early synsedimentary cementation (Cipriani et al., 2023, 2024).

The biogenic coralligenous structure serves as a captivating geobiological substrate, hosting a flourishing biodiversity. Cavities act as sediment traps further enhancing the potential biodiversity of the coralligenous. This diverse habitat, stemming from on the three-dimensional framework of the build-up remains largely unknown, as do the growth and modes patterns of its complex structures.

Despite the growing body of research on coralligenous, a series of fundamental questions remain. What are the modes and patterns of aggradation of the coralligenous and what taphonomic processes, involving the coralligenous framework and porosity distribution, affect this important geobiological substrate?

The analysis of the skeletal density and porosity of actively growing coralligenous provides insight into the taphonomy and early diagenetic processes of these structures and a key for interpreting their growth pattern and environmental context, fundamental to deciphering their fossil counterparts. Several investigations focused on the age and growth rate of these build-ups, showing that these structures can develop and live up to 5000–6000 years along the Mediterranean shelf (Sartoretto et al., 1996; Di Geronimo et al., 2002; Bertolino et al., 2017a; Basso et al., 2022; Varzi et al., 2023). Their accretion rate, defined as the algebraic sum between construction and erosion, range from 0.006 mm/yr^{-1} to 0.83 mm/yr^{-1}. Investigations on the internal architecture of the build-up have been seldom performed (Di Geronimo et al., 2002; Bertolino et al., 2017b; Basso et al., 2022; de Luca et al., 2023), however a timeline of the history of these bioconstructions remains elusive.

Additionally, analyses of the internal structure of the coralligenous reveal an extremely complex and non-linear structure, hinting to an intricated history of various taphonomic processes influencing framework density and porosity distribution. Computed Tomography (CT) scanning offers a non-invasive and highly detailed method for analysing complex three-dimensional structures such as fossilised bones (Ketcham and Carlson, 2001; Carlson et al., 2003; Mees et al., 2003) and geological features, (e.g., stalactites Zhang et al., 2010; Walczak et al., 2015) or biogenic nodules (Leal et al., 2012; Teichert, 2014; Torrano-Silva et al., 2015; Chandra et al., 2024) down to the extremely small foraminiferal scale (Coletti et al., 2018). Preliminary CT investigation of the composition, internal structure and density of build-ups collected offshore Marzamemi (SE Sicily) showed a complex framework and changes in density and porosity from the internal to the external parts (Bracchi et al., 2022). In this paper, the inner skeletal structure of four coralligenous build-ups collected along a depth gradient has been analysed by CT scanning. In addition, radiocarbon dating was performed on the build-ups to assess their age.

This work aims to fill knowledge gaps on coralligenous growth modes and models, delving into its complex structure and history, to identify understand potential factors that control and influence its development, reconstructing a possible timeframe of its evolution.

2. Materials and methods

2.1. Study area

The study area is located offshore the village of Marzamemi (Siracusa) on the southern part of the Hyblean plateau, in southeastern Sicily (Fig. 1).

The stratigraphic succession consists of carbonate sediments ranging from the upper Cretaceous to the Quaternary (Distefano et al., 2021). Near Marzamemi village, the lithology mainly comprises the Lower Pliocene Trubi Formation and the white-yellowish marls of the Upper Pliocene.These units represent the main source of the sediment drained into the adjacent basin.

Erosional subaerial processes have sculpted distinctive landforms

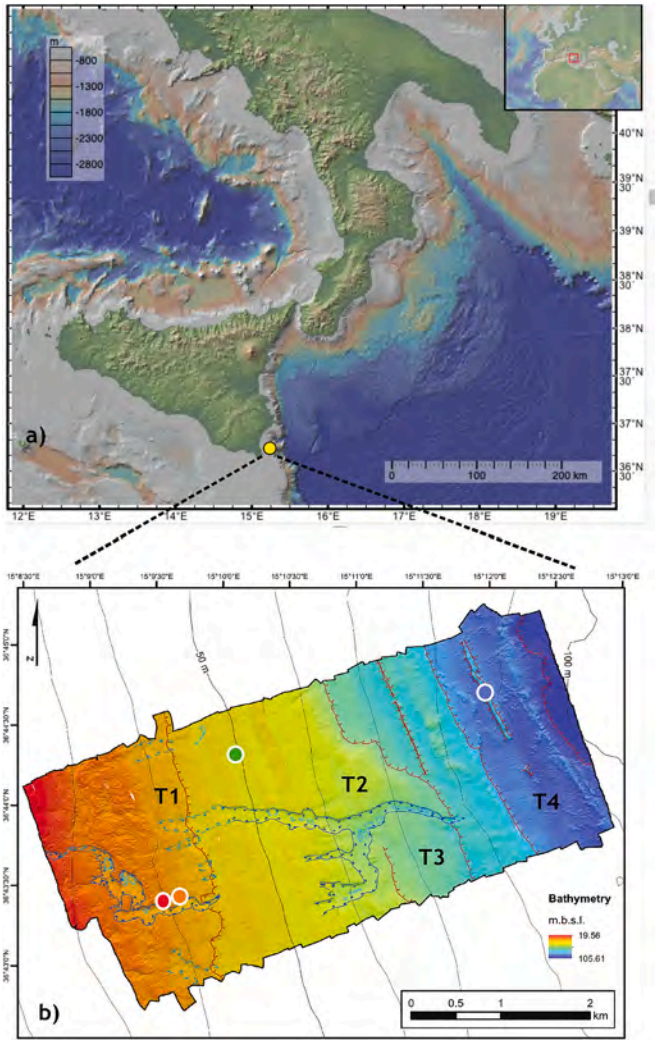

Fig. 1. Map of the Ionian Sea **(a)** with location of the study area off the Marzamemi coast (yellow dot) and bathymetric map of the study area (**b**). Coloured dots indicate the sites of build-up collection. Red: CBR2_3_7c; orange: CBR2_4_21c; green: CBR16_6c; blue: CBR9_57c. Red lines indicate the rims of submerged terraces (T1 to T4) and blue lines indicate the underwater canals (mod. From Varzi et al., 2023, 2024). (For interpretation of the references to colour in this figure legend, the reader is referred to the web version of this article.)

within the carbonate units of the plateau, now exposed in both emerged and submerged settings. In the sublittoral and inner shelf zones, relict karst depressions occur (Distefano et al., 2021; Varzi et al., 2023). Distinctive marks of subaerial erosional surfaces can be distinguished on the submerged morphology, including a series of four terrace rims now found at increasing depths and channels incised almost perpendicular to the coastline (Fig. 1). These features point to the low relative sea level caused by the interplay between regional uplift and eustatism during the Late Quaternary. Late Pleistocene marine terraces formed approximately 15 m above present-day sea level (Distefano et al., 2021). The following evolution produced sedimentary deposition and transformed river valleys into progressively infilling estuaries (Distefano et al., 2021).

The seafloor morphology of the relatively vast (17 km^2) study area, from which the samples were collected (Fig. 1), was described by Varzi et al. (2023). The topography is characterised by a succession of marine terraces likely associated with tectonic uplift events and transgressive/regressive phases during the Quaternary (Varzi et al., 2024). Notably, the coralligenous build-ups, distributed along the 36–42 m and 86–102

m isobaths, are linked with these terraces individuated by Varzi et al. (2024) (Table 1).

Following surveys with a Remotely Operated Vehicle (ROV, Bracchi et al., 2022; Varzi et al., 2023), four discrete build-ups (CBR2_3_7c, CBR2_4_21c, CBR16_6c and CBR9_57c) were selected and collected by professional SCUBA divers at 36.2, 36.7, 47.7 and 85 m of water depth (w.d.) (Fig. 1). All the samples and associated materials have been analysed and stored at the Department of Earth and Environmental Sciences of the University of Milano-Bicocca (Milan, Italy).

2.2. CT scan

After collection, the living cover of fleshy (non-building) organisms was manually removed (Fig. 2a and b, for comparison), as described in Bracchi et al. (2022), and the four build-ups were analysed with a CT apparatus. For this analysis we used the model RevolutionEVO integrated with the scanner PET/TC Discovery MI -General Electric, property of "Fondazione Tecnomed" of the University of Milano-Bicocca based at the Nuclear Medicine Department in Monza (Italy), with the following acquisition parameters: 140 kV and step 0.625 mm. The build-ups were scanned along their three main axes and the images were reconstructed using the axial filter "bone plus", in order to best visualise the carbonate fraction (Fig. 2b). The results yielded tomographic images of the build-ups, represented in greyscale to reflect the varying densities of the skeletal structure. Thresholded images were generated using the AMIRA-Avizo software by Thermo Fisher Scientific, in order to subdivide the continuous grey levels of density into discrete values. This elaboration facilitated the recognition and spatial distribution of the voids within the skeletal structure. Thresholded values were determined via software selection and adjusted using the grey levels data, delineating four materials of increasing density, as follows: Low-Density (LD), Medium-Density (MD), High-Density (HD) and Ultra High-Density (UHD) (Fig. 2c). Absolute porosity was calculated using the ratio between the total volume and the volume occupied by the voids.

For the analysis of morphological and physical variations among the different sections of the build-ups (i.e., the changes in porosity and the relative abundance of the thresholded materials), we employed the geometry tool of the Avizo software. This method entailed the virtual partition of discrete volumes inside the structure, enabling the analysis of the relative distribution of pores and materials within each volume (Fig. 3). Using the geometry tool of the Avizo software, virtual 3D cubic volumes (ca 125 cm^3) were drawn inside the skeletal structure, distributing the cubes from top to bottom of the build-ups (Fig. 3). Subsequently, the cubes were analysed for porosity and the relative abundances of the four materials, resulting in a series of graphs illustrating the changes in density and porosity alongside the primary vertical axis were produced. The dimensions of the cubes were selected to encompass the maximum volume of the build-up and ensure reproducibility between the four build-ups. Pores were identified and classified by the software based of their size, specifically, all the voids smaller than 256 mm were classified as pores. Larger voids were instead identified as cavities.

Table 1
List of the four investigated build-ups, with indication of depth and the coordinates of the collection site, as well as the position within the submarine terraces described by Varzi et al. (2024).

Build-ups	Water Depth	Coordinates	Terraces
CBR2_3_7c	36.2 m	36°43.394′ N 15°09.469′ E	T1
CBR2_4_21c	36.7 m	36°43.454′ N 15°09.657′ E	T1
CBR16_6c	47.7 m	36°43.82′ N 15°10.205′ E	T2
CBR9_57c	85 m	36°43.95′ N 15°10.210′ E	T4

After the CT scanning, each of the four build-ups was cut in two halves alongside their main vertical axis to allow a visual validation and description of the materials, all the various subsampling have been documented using a Nikon D3500 camera. To improve our interpretation of the correspondence between the four selected density classes and the coralligenous structure and components, thin sections of the selected areas of the build-ups were prepared in order to characterise the component occurrence and the microfacies. The description of the identified materials and porosities follows Flügel (2010). R statistical software and STATA software were used for the statistical analysis and data visualisation.

2.3. Build-ups general morphology

The main characteristics of the collected build-ups (Fig. 4) as reported in Table 1.

2.3.1. CBR2_3_7c

The CBR2_3_7c build-up (hereafter 7c), was collected at 36.2 m w.d. and is roughly columnar in shape (Fig. 4a). Upon collection it was 56 cm in height with a diameter measuring 19 cm at the base, rising to 37 cm at mid-height, and then tapering to 25 cm at the top (Bracchi et al., 2022). Notably, 7c coalesced, at its larger circumference, with the nearby build-ups (Fig. 4a). The 7c build-up was collected in a densely populated area with numerous interconnected build-ups covering the seafloor and appearing as a tabular structure (Bracchi et al., 2017).

2.3.2. CBR2_4_21c

The CBR2_4_21c build-up (hereafter 21c), was collected at 36.7 m w.d. and has a squat shape (Fig. 4b). At collection it was 38 cm in height with a maximum diameter of 112 cm. The 21c build-up was collected next to a submarine channel (Fig. 1), in an area with sandy coarse bottom and rhodoliths. Several other scattered build-ups occurred in the area (Fig. 4b).

2.3.3. CBR16_6c

The CBR16_6c build-up (hereafter 6c), was collected at 47.7 m w.d., and has a laterally compressed mushroom shape, with a thin columnar "foot" connecting the build-up to the seafloor and a large "head" on the top (Fig. 4c). At collection it measured 31 cm in height, the columnar foot was 12 cm in diameter while the larger upper portion had a main diameter of 27 cm. It was collected in a coarse sandy seafloor, characterised by high turbidity and dim light conditions (Fig. 4c). Build-ups were extremely scattered in the collection site, and apparently similar in dimension and shape to the 6c (Fig. 4c).

2.3.4. CBR9_57c

The CBR9_57c build-up (hereafter 57c), was collected at 85 m w.d. and has a compressed columnar shape, with two sides flat and large and the other two convex and very narrow. Two distinct outgrowths at the base of the build-up acted as supports, connecting the build-up to the seafloor (Fig. 4d). At collection 57c build-up was 25 cm high, with a maximum diameter of 23 cm. It originated from the deepest collection site, notably different from the others, characterised by almost total darkness and high turbidity (Fig. 4d). Build-ups in the area grew in clusters and were occasionally connected to each other (Fig. 4d).

2.4. Pores classification

Pores inside the build-ups were identified and classified on the basis of their size. Using the classification of Flügel (2010), we distinguished between small mesopores (between 0.06 and 0.5 mm), large mesopores (between 0.5 and 16 mm) and small megapores (between 16 and 32 mm).

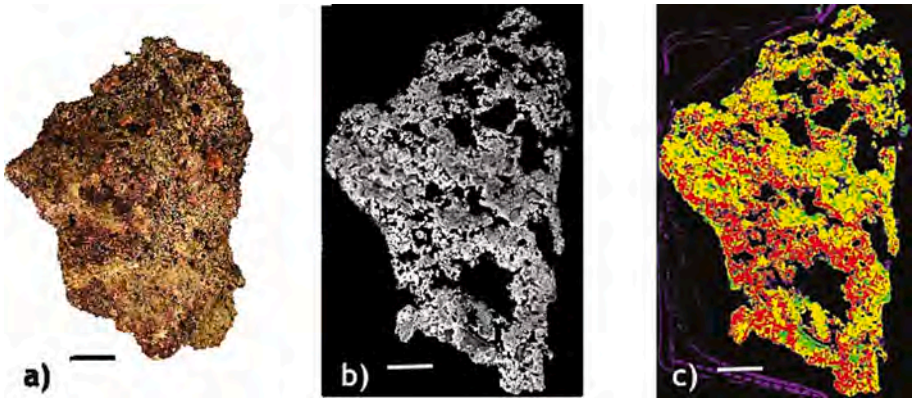

Fig. 2. **a**) CBR_7c buildup in life position; **b**) CT scan of the build-up, grey shading indicating density degrees of the material (the lighter the denser), note the high porosity (in black) of the structure; **c**) thresholded image of the CT scan. The continuous grey shadowing was thresholded in discrete values corresponding to colours: red = UHD, yellow = HD, green = MD, purple = LD. (For interpretation of the references to colour in this figure legend, the reader is referred to the web version of this article.)

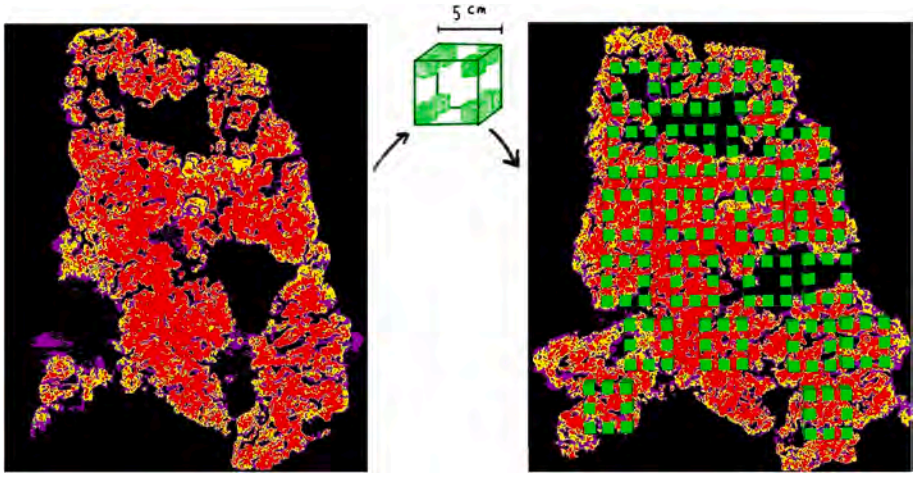

Fig. 3. Process of volume virtual cutting of the build-up. A series of virtual 3D boxes (in green) of ca 5 cm in size is drawn inside the thresholded image. The result is a series of 3D boxes inside the build-up, dividing the structure. (For interpretation of the references to colour in this figure legend, the reader is referred to the web version of this article.)

2.5. Radiocarbon dating

Radiocarbon dating was performed at the Milano-Bicocca University Centre for Dating and Archaeometry (CUDAM) on selected coralline algae fragments from the build-ups, after ascertaining the absence of diagenetic overprints and recrystallization. The fragments were selected on the basis of the density value identified throught the CT-analysis, with the aim of investigating the age of the HD and UHD densities, which constitute the hard crust of the algal build-up within the structures. Additionally, age differences across distinct zones within the build-ups were also investigated.

Samples for radiocarbon dating were collected from three build-ups, i.e. the shallowest 7c and 21c and the deepest 57c. The samples were preliminarily etched in a 0.1 M HCl solution to remove the outer layers, then rinsed three times in deionized water to neutralise the material. The samples were then chemically digested under vacuum using pure phosphoric acid, collecting the produced CO_2. The carbon dioxide was then transferred in a reactor and reduced to carbon powder via catalytic reaction. The isotopic concentration analysis was carried out at the CIRCE laboratory in Caserta, Italy, using a NEC 3MV tandem accelerator. The data were calibrated using the OxCal v.4.4.4 software (Ramsey, 2009) and the Marine20 curve (Heaton et al., 2020).

2.6. Microfacies and mineralogical analysis

The microfacies and mineralogical composition of the carbonate framework, of two representative build-ups (7c and 21c) were previously analysed in detail by Cipriani et al. (2023, 2024), and a synthesis of their results is here reported for contextual completeness. Thin sections were prepared from selected portions of each build-up and analysed under an optical microscope (Zeiss Axioplan 2 Imaging) at variable magnifications (2.5× to 40×). UV-epifluorescence microscopy was employed using high-performance filter sets (436/10 nm and 450–490 nm excitation; >470 nm and > 515 nm emission) to detect the presence and distribution of organic compounds, following the approach of Neuweiler et al. (2000, 2003, 2023). Selected fragments were further analysed using scanning electron microscopy (UHR-SEM, ZEISS Crossbeam 350) and energy-dispersive X-ray spectroscopy (EDS) for their micromorphological and compositional characterisation. Analyses were conducted under high vacuum with an accelerating voltage of 10–15 keV and live times of 30 s. Quantification was performed using a silicon drift detector (EDAX Octane Elite Plus), with reference to internal standards and processed via the APEX software suite (AMETEK, V2).

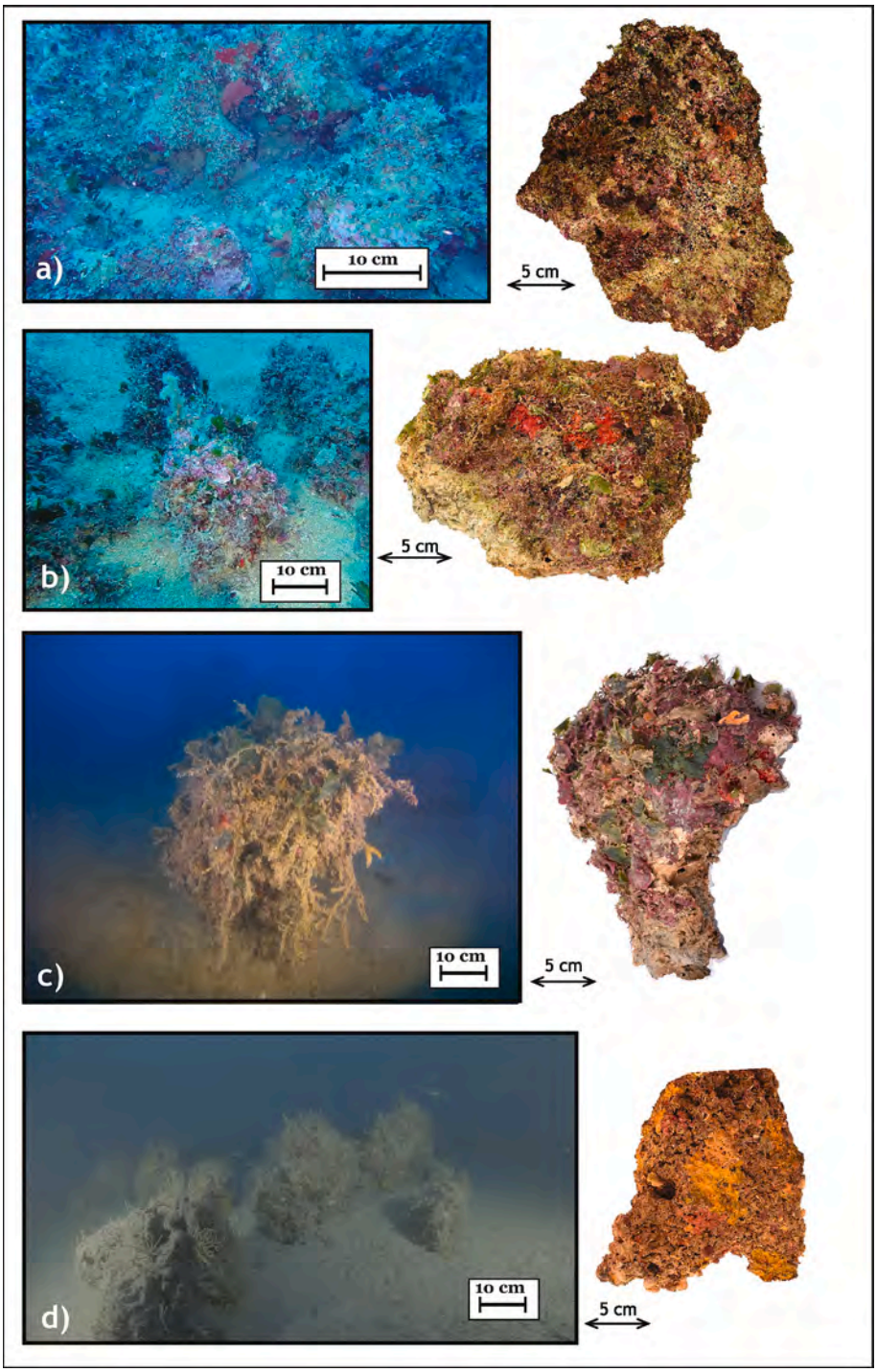

Fig. 4. Underwater photos of the analysed build-ups in their in-situ growth position (left) and after the scuba diver collection (right): (**a**)CBR2_3_7c; (**b**) CBR2_4_21c (**c**) CBR16_6c; and (**d**) CBR9_57c build-ups.

3. Results

3.1. Visual and mineralogical validation of constituting materials and density

Upon sectioning, the UHD material appears as a grey-brownish hard crust, with few or no pores visible to the naked eye (Fig. 5). The UHD material consists mainly of algal thalli and lithified sediment (Fig. 6a-d). SEM-EDS analyses confirmed the preservation of skeletal original mineralogy (high-Mg calcite and aragonite). However, the sediment showed moderate to extensive lithification. Lithified sediments were divided into two main types of autochthonous micrite: aphanitic and peloidal (Cipriani et al., 2023, 2024). Both types exhibit strong autofluorescence under UV light, indicating high organic content. SEM-EDS analysis showed that autochthonous micrite (consisting of fine anhedral to sub-euhedral crystals) showed a high-Mg calcite composition (Ca ~91 wt%, Mg ~6.5 wt%) and minimal detrital content (<2 wt%) (Cipriani et al., 2023, 2024).

HD material is composed of a grey-yellowish hard crust, with visible pores at the macro scale (Fig. 5). Thin section observation reveals the presence of algal thalli (Fig. 6c-f), bryozoans and serpulids and a moderate lithification degree. The HD material displays both growth

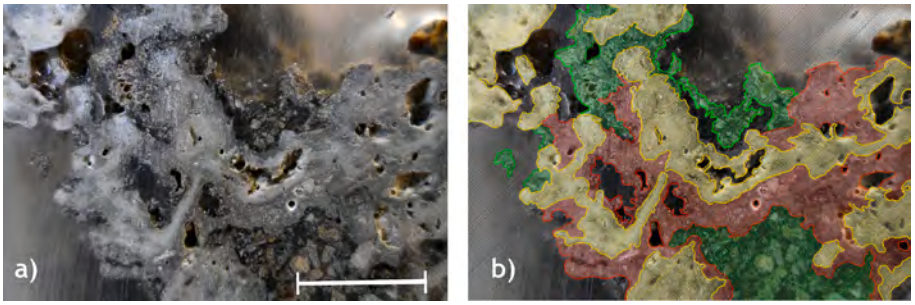

Fig. 5. Macro picture of a cut surface of the 7c build-up showing various constituent materials. **a**) Original Macro picture taken with a Nikon D3500 camera; **b**) interpreted and coloured material for comparison. Red: UHD, yellow: HD, green: MD. Scale bar 1 cm. (For interpretation of the references to colour in this figure legend, the reader is referred to the web version of this article.)

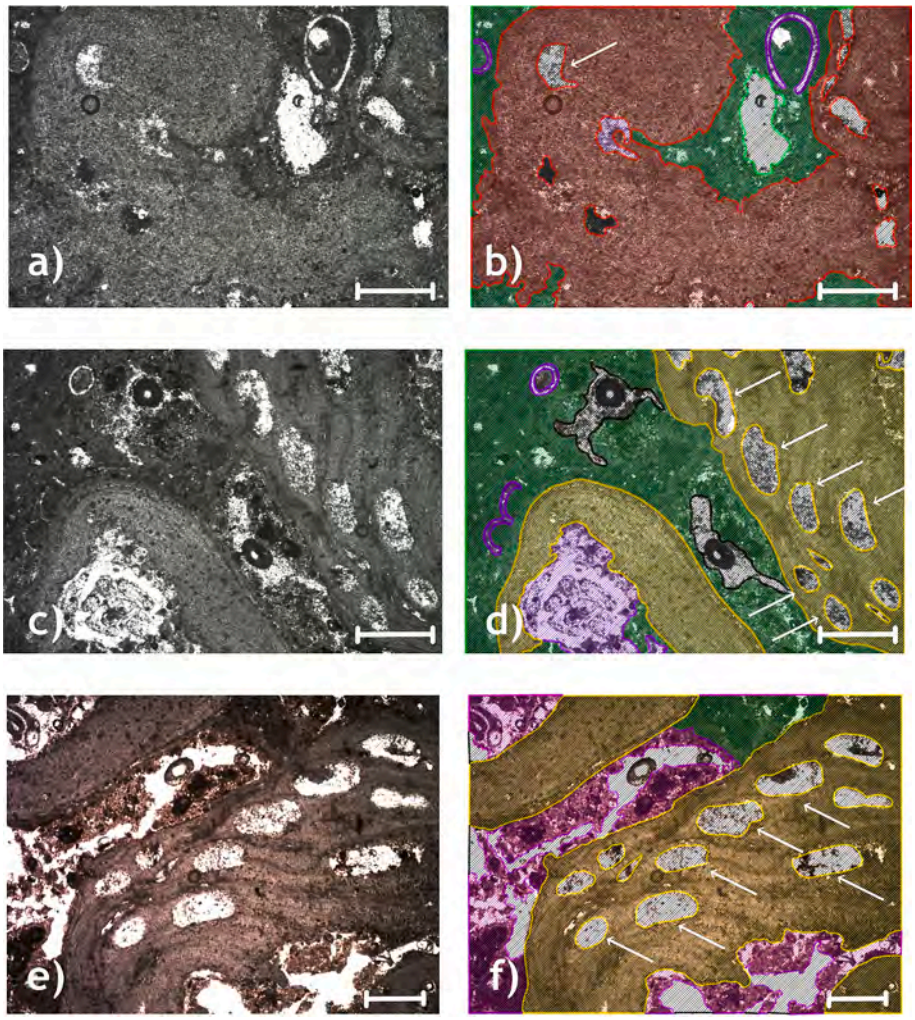

Fig. 6. Thin section images showing details of the various materials from the build-up 7c. **a), c), e)** microscope photographs at 20× magnification of the thin sections and **b), d), f**) interpreted and coloured material for comparison. Red: UHD, yellow: HD, green: MD, purple: LD; empty cavities are shown in white; white arrows indicate algal conceptacles. Scale bars, 0.5 mm. (For interpretation of the references to colour in this figure legend, the reader is referred to the web version of this article.)

framework porosity and boring porosity, with occasional sediment infilling (Fig. 5, Fig. 6c, d). Detrital micrite was subdivided into organic-rich and inorganic micrite based on texture and fluorescence evidence (Cipriani et al., 2023, 2024). SEM-EDS analysis showed detrital micrite (displaying a heterogeneous mineralogy and elevated terrigenous input) is composed of Ca (~46 wt%), Si (~26 wt%), Al (~12 wt%), and in minor amount of Fe (~6 wt%), and other elements (Mg, K, S, Na, Cl < 3 wt%).

MD material corresponds to compact dark-grey sediment inside larger cavities in the build-ups (Fig. 5). The sediment is made up of medium-to-fine sandy grains and bioclasts (Fig. 5, Fig. 6e, f).

LD material comprises different components of comparable density. This material consists of loose to poorly compacted sediment, typically nested inside large cavities of the build-ups. This sediment features mm-

sized bioclasts (mainly algal branches, but also includes ostracods, encrusting foraminifera and fragments of serpulids, bryozoan colonies and bivalves). These components are embedded within a fine-grained matrix rich in planktonic components (i.e., coccolithophores).

Given that MD and LD material largely consist of sediment, potentially introducing issues for radiocarbon dating, only the UHD and HD materials were selected for the radiocarbon dating.

Pores analysis reveals that the majority of pores fall into the small mesopores category, followed by the large megapores, while small megapores are less common (Fig. 7). The only exception is the 21c build-up, where small megapores occur more frequently than large ones.

3.2. Analysis of the build-ups

The CT-scan revealed a mean average porosity across the four build-ups of approximately 34 % (Table 2), with a minimum porosity of 26.2 % exhibited by the 21c build-up and a maximum of 41.6 % by the 6c build-up. Prominent cavities were present in all the build-ups. Build-up 7c showed several large cavities (cm-sized), primarily at its particularly porous and brittle top, but the largest one located at its bottom (Fig. 8a). The 21c build-up exhibited its largest cavity at its centre and further, smaller ones near its bottom (Fig. 8b). The 6c build-up showed a very large cavity crossing its entire upper half (Fig. 8c). Similarly, the 57c build-up featured a large cavity traversing its structure from top to bottom (Fig. 8d). In all the four build-ups, some of these cavities were connected to the outside, and contained loose sediment, and several boring, encrusting and opportunistic organisms dwelled inside.

The UHD material averaged around 41.7 % across the four build-ups (Table 2). However, its distribution varied, with 7c showing UHD mainly in the basal portion and at cavities edges (Fig. 8a), 21c having it concentrated at the top and sides (Fig. 8b), 6c exhibiting higher concentration at the bottom (Fig. 8c), and 57c showing the highest concentration of UHD among the four samples (57 %) (Table 2). The HD material averaged around 32.2 % (Table 2). The 7c was the build-up where the material was more abundant (42.5 %), and in the 21c it dominated the lower and middle portion of the structure (Fig. 8b). Build-up 6c showed a lower percentage of HD overall, with higher concentration at the top, while a thin layer of HD material surrounds the outermost portions of the 57c (Fig. 8c, d).

Table 2
Average percentage of the four materials and porosity of the four build-ups and the range of their calibrated age associated with the dated HD and UHD materials.

	7c (36.2 m wd)	21c (36.7 m wd)	6c (47.7 m wd)	57c (85 m wd)
LD	11.2 %	9.9 %	26 %	20.7 %
MD	13.7 %	12.8 %	3.8 %	2.4 %
HD	42.5 %	38.8 %	31 %	19.8 %
	500–1555 yrs. BP	2847 yrs. BP	N/A	935–1641 yrs. BP
UHD	32.4 %	38.4 %	45.3 %	57 %
	2021–2220 yrs. BP	3501–3871 yrs. BP	N/A	3336–5516 yrs. BP
Porosity	31 %	26.2 %	41.6 %	29.8 %

On average, MD and LD materials made up 7.4 % and 18.9 % respectively (Table 2). In the 7c build-up, LD and MD were primarily found at the top and within the lower parts of some cavities. For the 21c build-up, less dense materials were on the outside and inside some cavities. Notably, MD was almost entirely absent from the 6c and 57c build-ups. In 6c, LD material increased from bottom to top, while in 57c, it was concentrated on the surface, linked to a layer of serpulids (Fig. 9).

Radiocarbon dating indicates a maximum age of 5516 yrs. BP in the UHD portion of the 57c build-up, while the youngest recorded age, 500 yrs. BP, was found in the HD top portion of the 7c build up (Table 2).

4. Discussion

4.1. Porosity and density

The high porosity recorded inside the structure appears to be formed by various processes. Following Flügel (2010) three main types of porosity have been identified inside the investigated build-ups. A

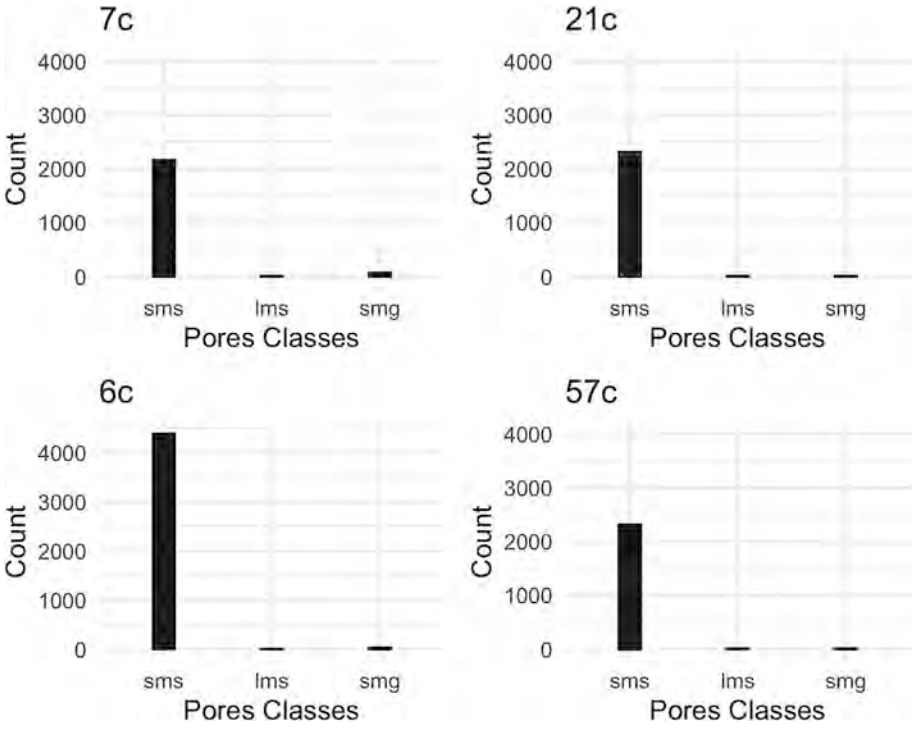

Fig. 7. distribution of the classes of pores in the four build-ups. Sms: small mesopores (between 0.06 and 0.5 mm); lms: large mesopores (between 0.5 and 16 mm); smg: small megapores (between 16 and 32 mm).

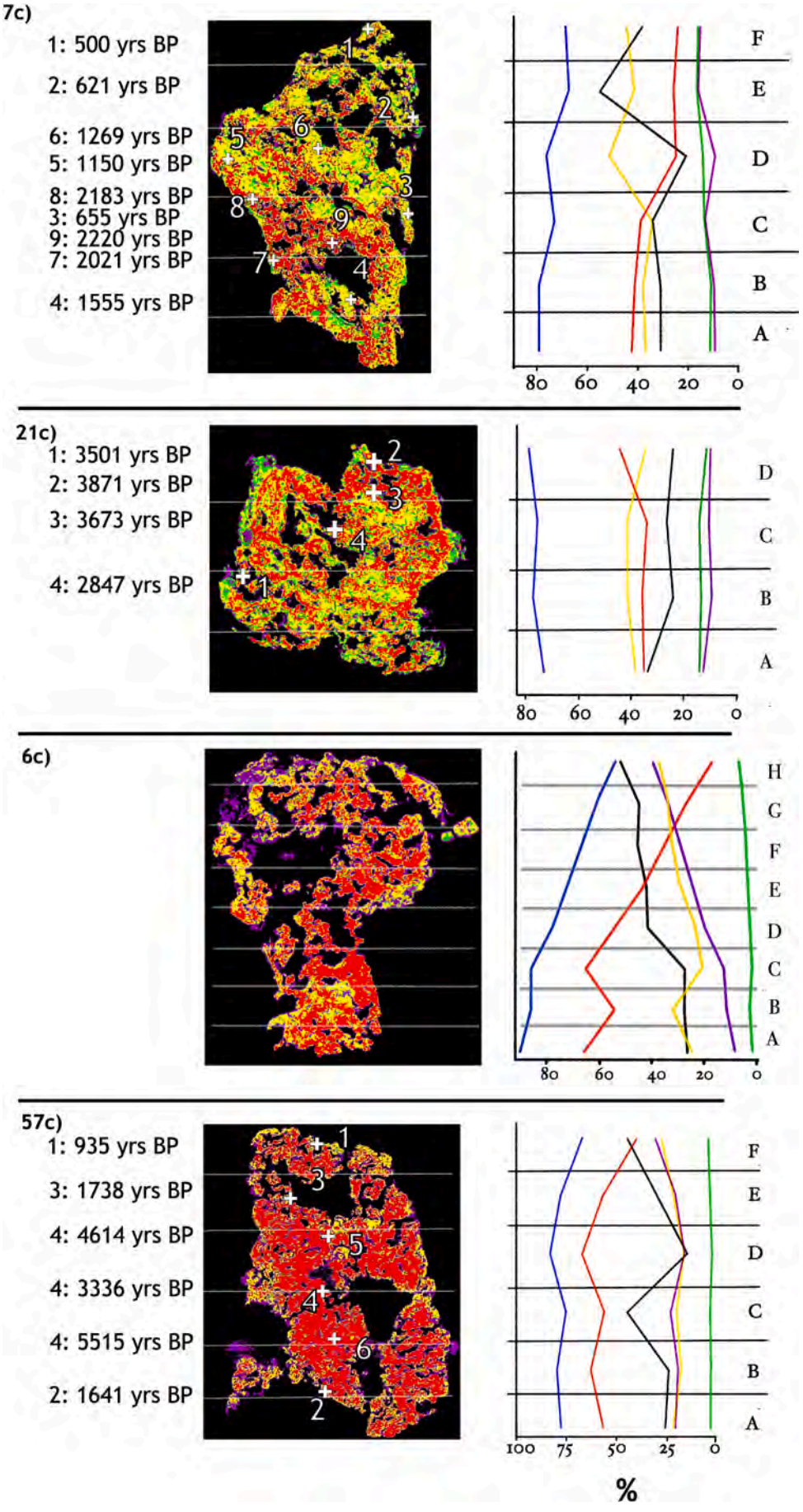

(caption on next page)

Fig. 8. Thresholded image of the four build-ups and variations in percentages of the four density materials with respect to the entire solid volume, and variations of the porosity throughout the build-ups. Blue line (HD + UHD), red line (UHD), yellow line (HD), green line (MD), purple line (LD), black line (Porosity). Porosity has been calculated as the ratio between the total volume and the volume occupied by the voids. White crosses indicate the sampling for radiocarbon dating with numbering in decreasing chronological order. (For interpretation of the references to colour in this figure legend, the reader is referred to the web version of this article.)

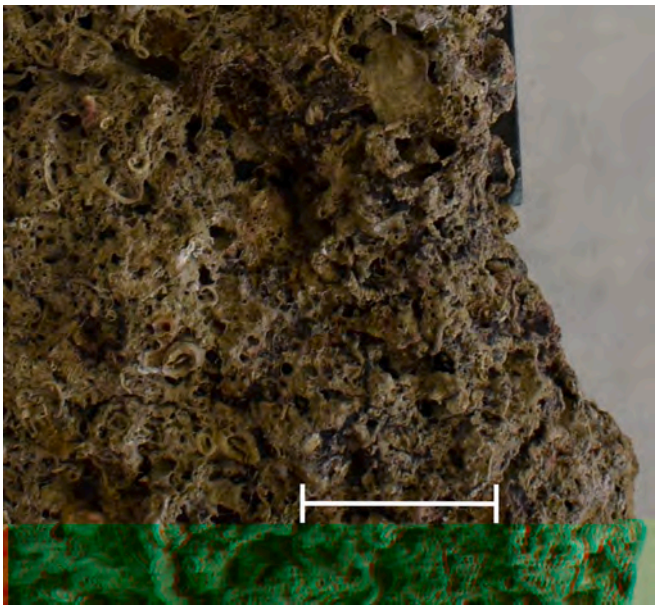

Fig. 9. Closeup image (taken with a Nikon D3500 camera) of the 57c surface. Note the dense layer of serpulids covering the surface. Scalebar: 1 cm.

"*primary porosity*", related to the intrinsic morphology of the skeletons of organisms forming the build-ups (e.g., algal conceptacles, bryozoans' zooidal cavities, annelids' tube lumens) and to the growth framework porosity (Choquette and Pray, 1970), created during the superposition and cementation of skeletons of the constituting organisms (i.e., spaces left between superposed algal thalli and skeletonised encrusters; spaces originally occupied by soft-bodied organisms lost after death and decomposition). A second type of porosity is "*bioerosional*", resulting from the activity of various micro- and macro-borers (e.g., cyanobacteria, sponges, mollusks).

The third and significant type of porosity is constituted by cavities of indeterminate and probably complex origin, which are ubiquitously present within the structures. These cavities could have been primary or bioerosional in their inception, and subsequently modified following multiple phases of filling, erosion, dissolution, and occupation or enlargement by animal dwellers. This type of porosity could fall into the "*enhanced porosity*" category of Flügel (2010), however, in our build-ups it may not exclusively derive from interparticle pores, and dissolution may not be the main process controlling its formation. Similarly, we refrain from employing the terms *constructional* and *destructional* voids, as proposed by Nitsch et al. (2015), as both constructive and destructive processes are involved in the origin of the voids observed in our build-ups.

The dense (HD) and very dense (UHD) materials that constitute the majority of the structure (comprising over 50 % in each build-up) appear to influence the characteristics of the pores. Analysis of the relationship between the total hard material (UHD and HD) and porosity reveals an inverse correlation, with an R^2 value of 0.53 across the build-ups (Fig. 10).

The lithification process seems to compact the material, transforming HD into UHD, thereby enhancing density and structural variability while simultaneously decreasing porosity. The formation of these build-ups results from the growth and accumulation of multiple generations of skeletonised organisms, coupled with the cementation of autochthonous micrite within cavities(Cipriani et al., 2024). Likely, this lithification process would involve the filling and subsequent cementation of the sediment inside small pores of the structure.

This hypothesis agrees with the behaviour of HD and UHD materials when compared to porosity: HD exhibits an inverse relationship with porosity in the shallower build-ups (7c and 21c), whereas in build-ups 57c and 6c, HD and porosity appear to correlate positively (Fig. 10). In these cases, both HD material and porosity are concentrated at the upper and external portions of the build-ups. Interestingly, the 57c build-up, in addition to the higher porosity at the top of its structure, has relatively high porosity on its most external portion as well, associated with less dense material (HD and LD, Fig. 8d). This high porosity appears to be related to annelid tube aggregations that extensively cover the external surface of the 57c build-up (Fig. 9). These organisms are known to associate with algal bioconstructions (Sanfilippo et al., 2011), indicating their preference for deep, dimly lit environments (Sanfilippo et al., 2013; Basso et al., 2022). Conversely, UHD material consistently shows an inverse relationship with porosity across all build-ups, except in the 7c build-up, where the pattern is less distinct ($R^2 = -0.03$). This observation suggests that the lithification process compacts HD material into denser UHD material, thereby reducing porosity and increasing the overall density.

In addition, all the build-ups are characterised by large cavities in the middle part of their structures, in apparent contrast with previously discussed porosity patterns. In particular, 7c features a prominent cavity on its side (Section B in Fig. 8, Fig. 11) that is likely the result of bioerosion by sponges that were observed at the time of collection (Cipriani et al., 2024), similarly to what has been reported on other Mediterranean build-ups (e.g., Bertolino et al., 2019; Teixidó et al., 2011). Both build-ups 6c and 57c present huge cavities crossing the entire structures, likely representing a more advanced developmental stage of the porosity (Fig. 8). This suggests that various stages of dismantling processes (mechanical and biological erosion, and dissolution) may occur at different depths and possibly during distinct temporal phases.

As for the other softer materials, the MD material is relatively abundant in the shallower 7c and 21c build-ups (13.7 % and 12.8 % respectively), while it is virtually absent from the deeper 6c and 57c build-ups. The LD material, on the other hand, is more abundant inside the 6c and 57c build-ups (22 % and 20.7 % respectively) while subordinate in the shallower 7c and 21c build-ups (11.2 % and 10.2 %, respectively). The difference of materials presence between the two shallower and the two deeper build-ups could suggest a difference in sedimentation exposure between the shallower and deeper areas. Sedimentation, both from terrigenous input from land, during discharge events (e.g., De Martini et al., 2010) and from a remobilization of present day bioclastic sediments, could preferentially affect the shallower sites, up to a certain distance from the coast. In particular, because the MD material is so poorly represented in the 6c build-up, despite the potentially high exposure to sedimentation of the area (the area is very near a submarine channel), can be explained by the fact that the 47 m w. d. area is dominated by finer material, and the coarser, land-derived material does not reach such depths and distances from the coast. In fact, analysis on the planktonic and molluscan assemblages inside the build-ups seems to suggest difference in the sedimentation regime of the studied area along an ideal coast-offshore gradient (Bazzicalupo et al., 2024; Bracchi et al., 2025).

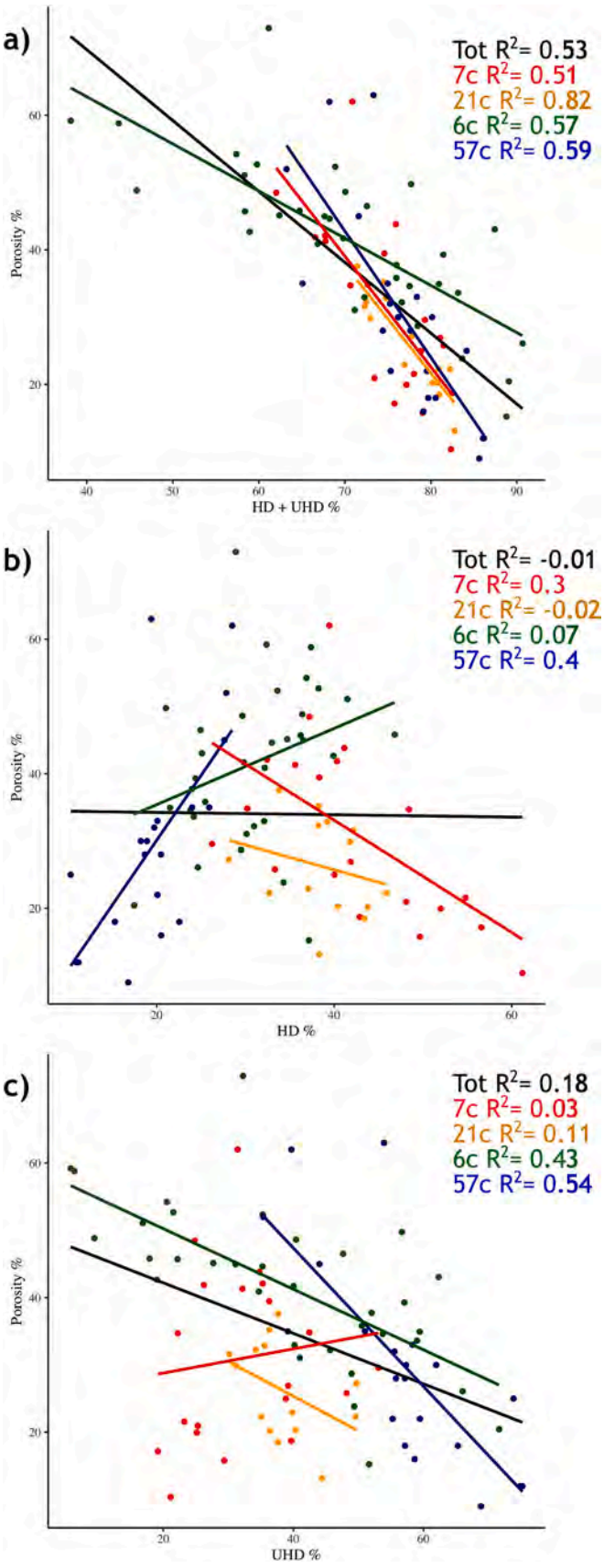

(caption on next column)

Fig. 10. Graphs of porosity v. the various hard material inside the studied build-ups. a) Porosity v. HD + UHD materials; b) Porosity v. HD material; c) Porosity v. UHD materials. Points represent the percentage values of the analysed cubes inside the build-ups, solid lines represent the regression line for the analysed values. Colours represent the various build-ups, black lines represent the totality of the build-ups (Red = 7c; Yellow = 21c; Green = 6c; Blue = 57c, Black line is the regression for the totality of the build-ups). (For interpretation of the references to colour in this figure legend, the reader is referred to the web version of this article.)

4.2. Age-density gradient

The inverse correlation between porosity and hard material (UHD and HD) content in the coralligenous build-ups suggests a gradual, syndepositional lithification process that likely occurred during the growth of these structures. The analysis indicates that the lithification process began at the inception of the build-ups and continued throughout their development, which explains why, in the analysed build-ups, the upper parts of the structures tend to exhibit more porosity and open cavities, whereas the lower sections are generally denser and more compact. This trend suggests that early lithification processes may have contributed to the cementation and stabilisation of the primary coralligenous skeletal framework, contributing to the consolidation of the structure (Cipriani et al., 2024).

The radiocarbon dating of materials within these build-ups allows for insight into the timeline of the lithification process. In the 7c build-up, the outermost HD material dates to between 650 and 500 years BP (placing it in the 14th to 15th centuries CE, during the early Renaissance period). In contrast, the older, internal HD material shows dates between 1500 and 1100 years BP (corresponding to the 4th to 6th centuries CE, a period coinciding with the decline of the Western Roman Empire). Even older UHD material in the midsection of the structure dates back to 2200–2000 years BP (spanning the transition from the Roman Republic to the Roman Empire). The 57c build-up reflects a similar but generally older age distribution. Its youngest material, located in small pockets at the edges of the structure, dates from 1730 to 990 years BP (corresponding to the early Roman Republic in the 3rd century BCE to the 10th century CE, during the growth of the Holy Roman Empire and the formation of the Kingdom of England). The UHD material in the 57c build-up's internal portions, however, is significantly older, dating back as much as 4000 to 5000 years BP (the end of the Neolithic period around 3000–2000 BCE). These dates suggest that the age of coralligenous reefs can extend over several millennia.

The observed age gradient between HD and UHD materials across build-ups points to a lithification timeline that spans roughly 1000 years for HD material to transform into the denser UHD form. Notably, an analysis of material abundances by depth reveals a pattern, with the percentage of HD material decreasing from 42.5 % in the shallowest 7c build-up, to 19.8 % in the deepest (57c build-up) (Fig. 12). Conversely, the UHD material exhibits an opposing trend, with its abundance increasing from 32.4 % in the shallowest 7c build-up to 57 % in the deepest structure (Fig. 12). This depth-gradient in material density indicates that as build-up depth increases, so does the degree of lithification.

The significance of this density and water depth gradient is reinforced by radiocarbon dates, where UHD materials consistently exhibit older ages than HD materials. The youngest UHD material, found in the 7c build-up, dates to approximately 2200 years BP, with older UHD materials in the 21c and 57c build-ups exceeding 3000 years in age, and the oldest material in the 57c reaching back 5500 years. Therefore, deeper and older build-ups are associated with a more extensive syndepositional lithification, occurring in the older portion of each build-up, while their surface is living and still growing.

Furthermore, none of the sampled build-ups displays a straightforward, linear growth pattern; instead, their development appears complex and likely influenced by various factors, including sedimentation

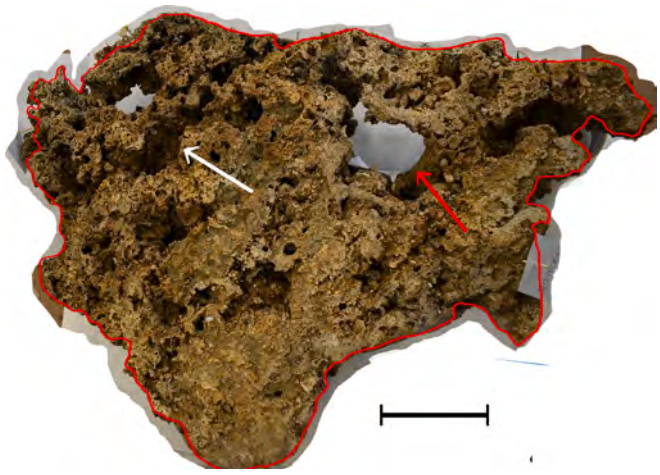

Fig. 11. Cross-section (contoured in red) of the 7c build-up, showing the porosity and the carbonate skeletal framework. Note the large cavity in the middle portion of the structure (red arrow) and the visible porosity in the upper part of the structure (white arrow). Scale bar = 10 cm. (For interpretation of the references to colour in this figure legend, the reader is referred to the web version of this article.)

and bioerosion, a characteristic feature of Mediterranean coralligenous reefs (Di Geronimo et al., 2001, 2002; Bertolino et al., 2017a; Basso et al., 2022).

The data indicates that the deepest build-up, 57c, has the oldest, densest material, while the shallowest build-up, 7c, contains a higher proportion of HD material and is comparably younger. Moreover, the 57c build-up may represent a later stage in coralligenous development, with a second phase of growth dominated by serpulids adapted to the low-light environments (Sanfilippo et al., 2013), hampering the algal growth (Basso et al., 2022). In contrast, the 7c build-up might represent an earlier stage in this development sequence, with less lithification due to its relatively younger age and shallower position. Thus, it can be hypothesised that, over time, the UHD content within the 7c structure may increase, following a trend similar to that observed in the deeper and older 57c build-up. This finding suggests that the depth-density gradient might rather be an age-density gradient, indicating that the 57c build-up likely started forming earlier than the others. This additional time for lithification processes may explain the gradual transformation from HD to UHD material, reflecting the consolidation and stabilisation of algal skeletal frameworks and sediment cementation over time.

The 21c build-up presents a puzzling age distribution, with its maximum calibrated age (3871 yrs. BP) falling between those of the 7c and 57c build-ups. This might suggest that that 21c may have been part of a larger, older coralligenous formation that fragmented and fell in a different position onto a new substrate, where growth resumed. This hypothesis is supported by the positioning of UHD material on the top of 21c, an unusual configuration with respect to the other build-ups. Furthermore, the timespan, provided by the radiocarbon dating, is far more compressed than in the other build-ups. In fact, the youngest age of the HD material inside the 21c is 2847 yrs. BP, while its oldest 3871 yrs. BP, inside the UHD material. This aligns with the 1000 yrs. timespan of the lithification, as stated before, but it also indicates the lack of ages spanning 500–2000 yrs., that were occurring in the other two dated build-ups. The isolated position within a submarine channel with high sedimentation cover (Bracchi et al., 2022) and the findings of sedimentological differences between the build-ups (Bazzicalupo et al., 2024) might suggest that environmental or hydrological shifts could have altered the growth direction also hampering the growth for a long timespan. However, it is more likely that 21c is a broken fragment issued from a nearby structure that was transported into the new position,

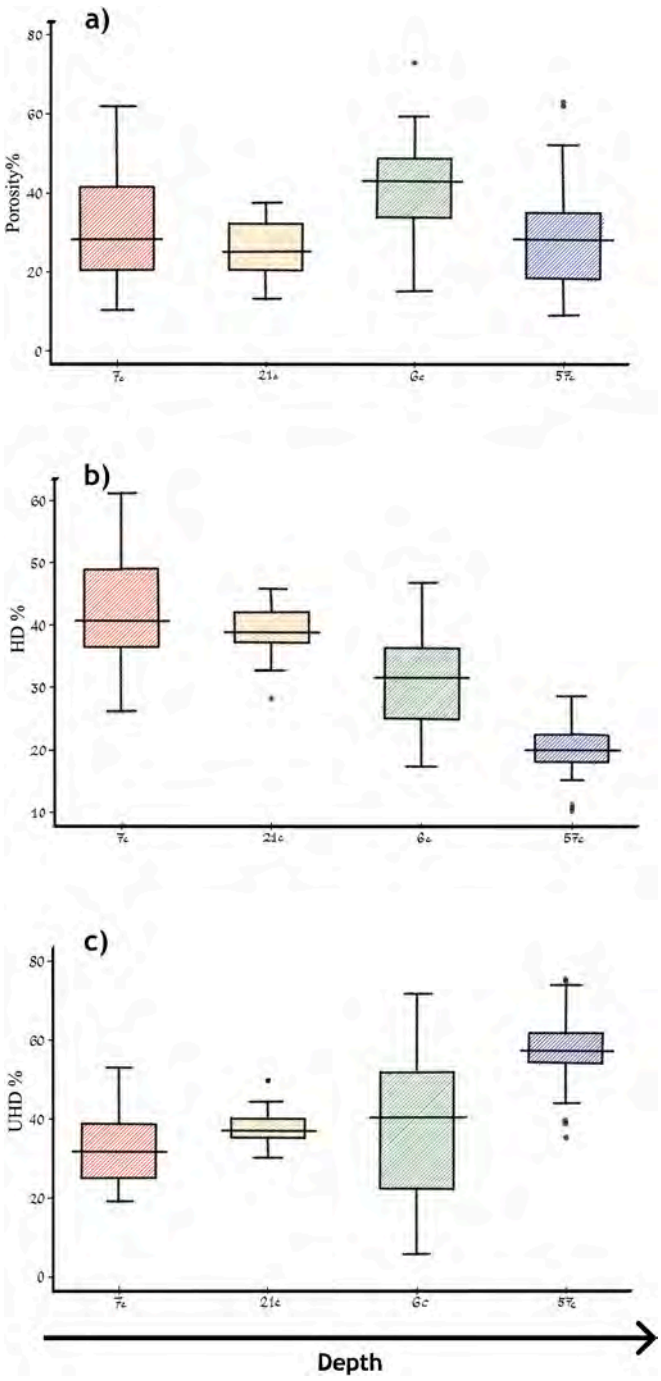

Fig. 12. Boxplot graph illustrating the percentage of porosity (a), HD (b) and UHD (c) materials of the four build ups. The boxplots are arranged following the depth increase from left to right (black arrow at the bottom of the image). Colour indicating the build-ups: Red = 7c; Yellow = 21c; Green = 6c; Blue = 57c. (For interpretation of the references to colour in this figure legend, the reader is referred to the web version of this article.)

possibly due to intense fishing activity in the area, as testified by the numerous piers and harbours dating back to the Magna Grecia Greek colonization(Scicchitano et al., 2008). The small size of 21c and the other surrounding build-ups also supports this hypothesis. In this sense, further analysis should focus on the substrate and age pattern of the surrounding build-ups.

4.3. Structure and depositional processes of the Coralligenous algal reef in a global context

The algal reefs occurring along the southeastern Sicily shelf off Marzamemi, as other algal reefs that have been investigated in the Mediterranean, developed within the photic zone during the Holocene sea-level rise. The related Holocene transgression progressively created suitable submarine conditions for the inception of the algal reefs by encrustation of the primary hard substrate, provided by a flight of underwater terraces under relatively stable tectonic conditions (Varzi et al., 2023, 2024; Fig. 1). Algal reef inception was therefore diachronic, with earliest marine transgression and algal reef accretion recorded by the deepest areas, in analogy with the strictly Holocene history of shelf colonization by tropical present-day coral reefs (Hynes et al., 2024). However, the present-day shallowest shelf areas off Marzamemi, down to about 30 m of water depth, are devoid of significant active algal bioconstruction, while the *Posidonia oceanica* seagrass meadows cover most of the seafloor (Varzi et al., 2023). This agrees with previous observations indicating that shallowest Mediterranean waters are unsuitable for coralligenous development, due to the dim-light preferences of Coralligenous coralline algae and the prevalence of fast-growing competitors for hard substrate occupation, such as light-loving seagrasses and seaweeds (Ballesteros, 2006; Burdett et al., 2012; Basso et al., 2022). It must be underlined that the Coralligenous habitat is ecologically and geologically very different from other coralline algal formations that have been confused with it, such as the intertidal "trottoir" or the unconsolidated rhodolith beds developing on sedimentary seafloors (e.g., Bosence, 1983; Georgiadis et al., 2009).

From the petrographic point of view, the studied algal build-ups represent an autochthonous carbonate-dominated rock supported by a rigid organic framework developed at the time of deposition, thus falling within the *framework* texture category (Ham, 1962; Lokier and Al Junaibi, 2016). Coralligenous algal reefs also conform the definition of *organic reef* (Riding, 2002) as essentially in place calcareous deposits created by sessile organisms. In particular, the superposition of algal thalli produces an *open frame reef*, where "cavities remain open during the early stages of reef growth and are occupied by cryptic encrusters, early cements and internal sediment; exposed skeleton encourages endoliths" (Riding, 2002).

The coralligenous build-ups of Marzamemi show a relief of up to 1 m above the surrounding sedimentary seabed (Varzi et al., 2023) and resist hydrodynamics, although waves seldom interact with the seafloor at >30 m of water depth. Marzamemi algal reefs have variable size, ranging from single columnar build-up <1 m (*microreef*; Riding, 2002), to a continuous cover >1000 m, as observed at the shallowest Marzamemi collection site (7c and 21c) where a *superreef* (sensu Riding, 2002) occurs.

Organic and skeletal growth, sedimentation rate, and early cementation are the most important constructional processes, that are offset by destructional processes such as bioerosion and physical breakage (Hubbard et al., 1990; Glynn and Manzello, 2015). These contrasting processes are continuously acting during reef growth (Riding, 2002) and the algebraic sum of the two opposed processes determines the actual reef accretion rates. This is particularly obvious when contrasting the internal portion with the most superficial layer of the 57c build-up, where enhanced bioerosion by internal borers (mainly sponges) and the extremely low cover of live coralline algae, partially substituted by annelid tubes, have significantly reduced the recent accretion rate of the deepest algal build-ups, among those investigated off Marzamemi.

Calculating a carbonate budget for the Mediterranean coralligenous algal reef requires dealing with a suite of information about builders' growth-rate, mechanical erosion, bioerosion, sediment production, and sediment transport across the shelf (Hubbard et al., 1990). While dozens of contributions are available for tropical coral reefs, only few and scattered data were devoted to this complex issue in the Mediterranean algal reefs (Sartoretto, 1998; Cerrano et al., 2001; Farber et al., 2016; Marchese et al., 2020), challenging future research efforts. Both the two main group of builders – colonial z-corals in the present-day tropical reefs vs. calcareous red coralline algae in the Mediterranean Coralligenous – possess clonal/modular characteristics that give them a higher morphological plasticity, larger size, long-life, and good building capacity, and both depend directly or indirectly on photosynthesis. Unluckily, climatic and oceanographic settings, depth distribution, geochemical environment, coralline algae ecology and sedimentary dynamics interacting with the mesophotic temperate Mediterranean algal reefs do not allow the straightforward import of tropical coral reef knowledge, despite the above mentioned petrographic and sedimentological analogies.

5. Conclusions

This study provides a comprehensive analysis of porosity, density, lithification, and age within four coralligenous build-ups from Marzamemi (Sicily), providing new insights into the formation and development of Mediterranean coralligenous reefs. Our results indicate that porosity within these structures arises from diverse origins, including primary framework porosity, bioerosional processes, and widespread enhanced porosity. The build-up structures are primarily composed of dense (HD) and very dense (UHD) calcareous materials, predominantly derived from algal thalli, with an observed inverse correlation between porosity and material density, emphasising the role of lithification in increasing structural rigidity.

Radiocarbon dating demonstrates an internal age gradient within the build-ups, with UHD material consistently predating HD material. The findings suggest a lithification timeline of approximately 1000 years for HD material to gradually transform into UHD. This age-related transformation follows a depth-density trend, with the proportion of UHD material increasing in deeper build-ups. These observations reveal that coralligenous build-ups undergo complex, non-linear growth influenced by environmental changes, sediment deposition, and bioerosion. Specifically, the deepest examined structure, the 57c build-up, exhibits significant lithification and extended UHD content, suggesting extensive structural cementation and advanced age. Conversely, the shallowest build-up, the 7c, appears to represent an earlier stage in lithification, with comparatively lower UHD content and younger ages of its material. This pattern suggests a potential depth-density gradient and an evolutionary trajectory of coralligenous build-ups in similar environments. The anomalous age distribution and internal density patterns within the 21c build-up seems to suggest that it may have been transported and resettled, potentially from a larger structure, possibly due to fishing activity in the area.

Overall, these findings enhance our understanding of coralligenous reef formation, geobiological development, and early lithification processes, shedding light on their potential resilience and responses to environmental changes.

CRediT authorship contribution statement

Pietro Bazzicalupo: Writing – original draft, Visualization, Methodology, Investigation, Formal analysis, Data curation, Conceptualization. **Valentina Alice Bracchi:** Writing – review & editing, Validation, Resources, Methodology, Conceptualization. **Mara Cipriani:** Writing – review & editing, Validation. **Adriano Guido:** Writing – review & editing, Validation. **Antonietta Rosso:** Writing – review & editing, Validation, Funding acquisition. **Rossana Sanfilippo:** Writing – review & editing. **Francesco Maspero:** Validation, Formal analysis. **Anna Galli:** Formal analysis. **Elena de Ponti:** Formal analysis. **Daniela Basso:** Writing – review & editing, Validation, Supervision, Project administration, Funding acquisition, Conceptualization.

Declaration of competing interest

The authors declare that they have no known competing financial interests or personal relationships that could have appeared to influence the work reported in this paper.

Acknowledgments

This work was funded by the Italian Ministry of Research and University Fondo Integrativo Speciale per la Ricerca (FISR). Project FISR2019 04543 “CRESCIBLUREEF - Grown in the blue: new technologies for knowledge and conservation of Mediterranean reefs”, within the framework of the Eu ropean Blue Growth strategy. This is the Catania Paleontological Research Group contribution n.528. The authors thank Mr. Nunzio Pietralito and the SUTTAKKUA diving school (Pachino, SR) for the retrieval of the samples and their support in the field activities. The authors thank Dr. Mauro Pietro Negri (University of Milano-Bicocca), for his help whit handling and sampling of the material. The authors thank Dr. Nicoletta Fusi (University of Milano-Bicocca) for her help with the Avizo Software analyisis. The authors thank the company “Marmi Airoldi” (Rescaldina, MI), for the help in cutting the build-ups.

Data availability

The data that support the findings of this study are available at this link: https://drive.google.com/file/d/1mMK_rpPw2QXWb8WGOJJsX9MNYqb-Lbln/view?usp=sharing

References

Ballesteros, E., 2006. Mediterranean coralligenous assemblages: a synthesis of present knowledge. An Annu. Rev. 44, 123–195.

Basso, D., Bracchi, V.A., Bazzicalupo, P., Martini, M., Maspero, F., Bavestrello, G., 2022. Living coralligenous as geo-historical structure built by coralline algae. Front. Earth Sci. 10. https://doi.org/10.3389/feart.2022.961632.

Bazzicalupo, P., Cipriani, M., Guido, Adriano, Bracchi, Valentina Alice, Rosso, Antonietta, Basso, Daniela, Guido, A., Bracchi, V.A., Rosso, A., Basso, D., 2024. Calcareous nannoplankton inside coralligenous build-ups: the case of Marzamemi (SE, Sicily). Bollettino Della Soc. Paleontol. Ital. 63. https://doi.org/10.4435/BSPI.2024.09.

Bertolino, M., Cattaneo-Vietti, R., Costa, G., Pansini, M., Fraschetti, S., Bavestrello, G., 2017a. Have climate changes driven the diversity of a Mediterranean coralligenous sponge assemblage on a millennial timescale? Palaeogeogr. Palaeoclimatol. Palaeoecol. 487, 355–363. https://doi.org/10.1016/j.palaeo.2017.09.020.

Bertolino, M., Costa, G., Carella, M., Cattaneo-Vietti, R., Cerrano, C., Pansini, M., Quarta, G., Calcagnile, L., Bavestrello, G., 2017b. The dynamics of a Mediterranean coralligenous sponge assemblage at decennial and millennial temporal scales. PLoS ONE 12, 1–19. https://doi.org/10.1371/journal.pone.0177945.

Bertolino, M., Costa, G., Cattaneo-Vietti, R., Pansini, M., Quarta, G., Calcagnile, L., Bavestrello, G., 2019. Ancient and recent sponge assemblages from the Tyrrhenian coralligenous over millennia (Mediterranean Sea). Facies 65. https://doi.org/10.1007/s10347-019-0573-4.

Bosence, D.W.J., 1983. Coralline algal reef frameworks. J. Geol. Soc. Lond. 140, 365–376. https://doi.org/10.1144/gsjgs.140.3.0365.

Bracchi, V.A., Basso, D., Marchese, F., Corselli, C., Savini, A., 2017. Coralligenous morphotypes on subhorizontal substrate: a new categorization. Cont. Shelf Res. 144, 10–20. https://doi.org/10.1016/j.csr.2017.06.005.

Bracchi, V.A., Bazzicalupo, P., Fallati, L., Varzi, A.G., Savini, A., Negri, M. Pietro, Rosso, A., Sanfilippo, R., Guido, A., Bertolino, M., Costa, G., De Ponti, E., Leonardi, R., Muzzupappa, M., Basso, D., San, R., Muzzupappa, M., Basso, D., 2022. The main builders of Mediterranean coralligenous : 2D and 3D quantitative approaches for its identification. Front. Earth Sci. 10, 1–12. https://doi.org/10.3389/feart.2022.910522.

Bracchi, V.A., Negri, M. Pietro, Bazzicalupo, P., Bertolino, M., Cipriani, M., Donato, G., Guido, A., Rosso, A., Sanfilippo, R., Sciuto, F., Basso, D., 2025. Mollusk diversity of coralligenous build-ups in the southwestern Ionian Sea. Mediterr. Mar. Sci. https://doi.org/10.12681/mms.38878.

Burdett, H.L., Hennige, S.J., Francis, F.T.Y., Kamenos, N.A., 2012. The photosynthetic characteristics of red coralline algae, determined using pulse amplitude modulation (PAM) fluorometry. Bot. Mar. 55, 499–509. https://doi.org/10.1515/BOT-2012-0135/MACHINEREADABLECITATION/RIS.

Cardone, F., Corriero, G., Longo, C., Pierri, C., Gimenez, G., Gravina, M.F., Giangrande, A., Lisco, S., Moretti, M., De Giosa, F., Mercurio, M., Marzano, C.N., 2022. A system of marine animal bioconstructions in the mesophotic zone along the Southeastern Italian coast. Front. Mar. Sci. 9. https://doi.org/10.3389/fmars.2022.948836.

Carlson, W.D., Rowe, T., Ketcham, R.A., Colbert, M.W., 2003. Applications of high-resolution X-ray computed tomography in petrology, meteoritics and palaeontology. Geol. Soc. Spec. Publ. 215, 7–22. https://doi.org/10.1144/GSL.SP.2003.215.01.02.

Cerrano, C., Bavestrello, G., Bianchi, C.N., Calcinai, B., Cattaneo-Vietti, R., Morri, C., Sarà, M., 2001. The role of sponge bioerosion in mediterranean coralligenous accretion. Mediterr. Ecosyst. 235–240. https://doi.org/10.1007/978-88-470-2105-1_30.

Chandra, V., Sicat, R., Benzoni, F., Vahrenkamp, V., Bracchi, V., 2024. A novel multi-scale µCT characterization method to quantify biogenic carbonate production. Geosci. Front. 15, 101883. https://doi.org/10.1016/J.GSF.2024.101883.

Choquette, P.W., Pray, L.C., 1970. Geologic nomenclature and classification of porosity in sedimentary carbonates. Am. Assoc. Pet. Geol. Bull. 54, 207–250. https://doi.org/10.1306/5D25C98B-16C1-11D7-8645000102C1865D.

Cipriani, M., Basso, D., Bazzicalupo, P., Bertolino, M., Bracchi, V.A., Bruno, F., Costa, G., Dominici, R., Gallo, A., Muzzupappa, M., Rosso, A., Perri, F., Sanfilippo, R., Sciuto, F., Guido, A., 2023. The role of non-skeletal carbonate component in Mediterranean Coralligenous: new insight from the CRESCIBLUREEF project. Rend. Online Soc. Geol. Ital. 59, 75–79. https://doi.org/10.3301/ROL.2023.12.

Cipriani, M., Apollaro, C., Basso, D., Bazzicalupo, P., Bertolino, M., Bracchi, V.A., Bruno, F., Costa, G., Dominici, R., Gallo, A., Muzzupappa, M., Rosso, A., Sanfilippo, R., Sciuto, F., Vespasiano, G., Guido, A., 2024. Origin and role of non-skeletal carbonate in coralligenous build-ups: new geobiological perspectives in biomineralization processes. Biogeosciences 21, 49–72. https://doi.org/10.5194/bg-21-49-2024.

Coletti, G., Stainbank, S., Fabbrini, A., Spezzaferri, S., Foubert, A., Kroon, D., Betzler, C., 2018. Biostratigraphy of large benthic foraminifera from Hole U1468A (Maldives): a CT-scan taxonomic approach. Swiss J. Geosci. 111, 495–508. https://doi.org/10.1007/s00015-018-0306-7.

Corriero, G., Pierri, C., Mercurio, M., Nonnis Marzano, C., Onen Tarantini, S., Gravina, M.F., Lisco, S., Moretti, M., De Giosa, F., Valenzano, E., Giangrande, A., Mastrodonato, M., Longo, C., Cardone, F., 2019. A Mediterranean mesophotic coral reef built by non-symbiotic scleractinians. Sci. Rep. 9, 1–17. https://doi.org/10.1038/s41598-019-40284-4.

de Luca, A., Lisco, S., Acquafredda, P., Gimenez, G., Moretti, M., 2023. The coralligenous in the present-day system from the Salento coast (southern Adriatic Sea). Rend. Online Soc. Geol. Ital. 59. https://doi.org/10.3301/ROL.2023.16.

De Martini, P.M., Barbano, M.S., Smedile, A., Gerardi, F., Pantosti, D., Del Carlo, P., Pirrotta, C., 2010. A unique 4000 year long geological record of multiple tsunami inundations in the Augusta Bay (eastern Sicily, Italy). Mar. Geol. 276, 42–57. https://doi.org/10.1016/J.MARGEO.2010.07.005.

Di Geronimo, I., Di Geronimo, R., Improta, S., Rosso, A., Sanfilippo, R., 2001. Preliminary observations on a columnar coralline build-up from off SE Sicily. Biol. Mar. Mediterr. 8, 229–237.

Di Geronimo, I., Di Geronimo, R., Rosso, A., Sanfilippo, R., Di Geronimo, I., Di Geronimo, R., Rosso, A., Sanfilippo, R., Di Geronimo, I., Di Geronimo, R., Rosso, A., Sanfilippo, R., 2002. Structural and taphonomic analysis of a columnar coralline algal build-up from SE Sicily. Geobios 35, 86–95. https://doi.org/10.1016/S0016-6995(02)00050-5.

Distefano, S., Gamberi, F., Baldassini, N., Di Stefano, A., 2021. Quaternary evolution of coastal plain in response to sea-level changes: example from South-East Sicily (Southern Italy). Water (Basel) 13, 1524. https://doi.org/10.3390/w13111524.

Donato, G., Sanfilippo, R., Basso, D., Bazzicalupo, P., Bertolino, M., Bracchi, V.A., Rosso, A., 2024. Biodiversity associated with a coralligenous build-up off Sicily (Ionian Sea). Regional Studies in Marine Science 80, 103868.

Farber, C., Titschack, J., Hanna Lydia Schönberg, C., Ehrig, K., Boos, K., Baum, D., Illerhaus, B., Asgaard, U., Bromley, R.G., Freiwald, A., Wisshak, M., 2016. Long-term macrobioerosion in the Mediterranean Sea assessed by micro-computed tomography. Biogeosciences 13, 3461–3474. https://doi.org/10.5194/BG-13-3461-2016.

Ferrigno, F., Rendina, F., Sandulli, R., Russo, G.F., 2023. Coralligenous assemblages: research status and trends of a key Mediterranean biodiversity hotspot through bibliometric analysis. Ecol. Quest. 35. https://doi.org/10.12775/EQ.2024.002.

Flügel, E., 2010. Diagenesis, porosity, and dolomitization. In: Microfacies of Carbonate Rocks. Springer, Berlin Heidelberg, pp. 267–338. https://doi.org/10.1007/978-3-642-03796-2_7.

Georgiadis, M., Papatheodorou, G., Tzanatos, E., Geraga, M., Ramfos, A., Koutsikopoulos, C., Ferentinos, G., 2009. Coralligène formations in the eastern Mediterranean Sea: Morphology, distribution, mapping and relation to fisheries in the southern Aegean Sea (Greece) based on high-resolution acoustics. J. Exp. Mar. Biol. Ecol. 368, 44–58. https://doi.org/10.1016/j.jembe.2008.10.001.

Glynn, P.W., Manzello, D.P., 2015. Bioerosion and coral reef growth: A dynamic balance. In: Coral Reefs in the Anthropocene. Springer, Netherlands, pp. 67–97. https://doi.org/10.1007/978-94-017-7249-5_4.

Ham, W.E., 1962. Classification of Carbonate Rocks—A Symposium. https://doi.org/10.1306/M1357.

Heaton, T.J., Köhler, P., Butzin, M., Bard, E., Reimer, R.W., Austin, W.E.N., Bronk Ramsey, C., Grootes, P.M., Hughen, K.A., Kromer, B., Reimer, P.J., Adkins, J., Burke, A., Cook, M.S., Olsen, J., Skinner, L.C., 2020. Marine20—the marine radiocarbon age calibration curve (0–55,000 cal BP). Radiocarbon 62, 779–820. https://doi.org/10.1017/RDC.2020.68.

Hubbard, D.K., Miller, A.I., Scaturo, D., 1990. Production and cycling of calcium carbonate in a shelf-edge reef system (St. Croix, U.S. Virgin Islands); applications to the nature of reef systems in the fossil record. J. Sediment. Res. 60, 335–360. https://doi.org/10.1306/212F9197-2B24-11D7-8648000102C1865D.

Hynes, M.G., O'Dea, A., Webster, J.M., Renema, W., 2024. RADReef: a global holocene reef rate of accretion dataset. Sci Data 11, 1–11. https://doi.org/10.1038/s41597-024-03228-w.

Ketcham, R.A., Carlson, W.D., 2001. Acquisition, optimization and interpretation of X-ray computed tomographic imagery: applications to the geosciences. Comput. Geosci. 27, 381–400. https://doi.org/10.1016/S0098-3004(00)00116-3.
Laborel, J., 1961. La concretionnement algal "coralligene" et son importance geomorphologique en mediterranee. 23, 37-60 Rec. Trav. St. Mar. End. Bull.
Laborel, J., 1987. Marine biogenic constructions in the Mediterranean – a review. Sci. Rep. Port-Cros Natl. Park 97–126.
Leal, R.N., Bassi, D., Posenato, R., Amado-Filho, G.M., 2012. Tomographic analysis for bioerosion signatures in shallow-water rhodoliths from the Abrolhos Bank, Brazil. J. Coast. Res. 28, 306–309. https://doi.org/10.2112/11T-00006.1.
Lokier, S.W., Al Junaibi, M., 2016. The petrographic description of carbonate facies: are we all speaking the same language? Sedimentology 63, 1843–1885. https://doi.org/10.1111/SED.12293.
Marchese, F., Bracchi, V.A., Lisi, G., Basso, D., Corselli, C., Savini, A., 2020. Assessing fine-scale distribution and volume of Mediterranean algal reefs through terrain analysis of multibeam bathymetric data. A case study in the Southern Adriatic continental shelf. Water (Switzerland) 12. https://doi.org/10.3390/w12010157.
Mees, F., Swennen, R., Van Geet, M., Jacobs, P., 2003. Applications of X-ray computed tomography in the geosciences. Geol. Soc. Spec. Publ. 215, 1–6. https://doi.org/10.1144/GSL.SP.2003.215.01.01.
Neuweiler, F., Rutsch, M., Geipel, G., Reimer, A., Heise, K.H., 2000. Soluble humic substances from in situ precipitated microcrystalline calcium carbonate, internal sediment, and spar cement in a cretaceous carbonate mud-mound. Geology 28, 851–854. https://doi.org/10.1130/0091-7613(2000)28<851:SHSFIS>2.0.CO;2.
Neuweiler, F., d'Orazio, V., Immenhauser, A., Geipel, G., Heise, K.H., Cocozza, C., Miano, T.M., 2003. Fulvic acid–like organic compounds control nucleation of marine calcite under suboxic conditions. Geology 31, 681–684. https://doi.org/10.1130/G19775.1.
Neuweiler, F., Kershaw, S., Boulvain, F., Matysik, M., Sendino, C., McMenamin, M., Munnecke, A., 2023. Keratose sponges in ancient carbonates – a problem of interpretation. Sedimentology 70, 927–968. https://doi.org/10.1111/sed.13059.
Nitsch, F., Nebelsick, J.H., Bassi, D., 2015. Constructional and destructional patterns - Void classification of rhodoliths from Giglio Island, Italy. Palaios 30, 680–691. https://doi.org/10.2110/palo.2015.007.
Pérès, J.M., 1982. Major benthic assemblages. Mar. Ecol. 5, 373–522.
Piazzi, L., Gennaro, P., Balata, D., 2012. Threats to macroalgal coralligenous assemblages in the Mediterranean Sea. Mar. Pollut. Bull. 64, 2623–2629. https://doi.org/10.1016/J.MARPOLBUL.2012.07.027.
Piazzi, L., Ferrigno, F., Guala, I., Cinti, M.F., Conforti, A., De Falco, G., De Luca, M., Grech, D., La Manna, G., Pascucci, V., Pansini, A., Pinna, F., Pireddu, L., Puccini, A., Russo, G.F., Sandulli, R., Santonastaso, A., Simeone, S., Stelletti, M., Stipcich, P., Ceccherelli, G., 2022. Inconsistency in community structure and ecological quality between platform and cliff coralligenous assemblages. Ecol. Indic. 136, 108657. https://doi.org/10.1016/J.ECOLIND.2022.108657.
Ramsey, C.B., 2009. Bayesian analysis of radiocarbon dates. Radiocarbon 51, 337–360. https://doi.org/10.1017/S0033822200033865.
Riding, R., 2002. Structure and composition of organic reefs and carbonate mud mounds: concepts and categories. Earth Sci. Rev. 58, 163–231. https://doi.org/10.1016/S0012-8252(01)00089-7.
Rosso, A., Sanfilippo, R., 2009. The Contribution of Bryozoans y and Serpuloideans p to Coralligenous Concretions From SE Sicily. First Mediterranean Symposium on the Coralligenous and Other Calcareous Bioconcretions of the Mediterranean Sea, pp. 1–36.
Rosso, A., Donato, G., Sanfilippo, R., Serio, D., Sciuto, F., D'Alpa, F., Bracchi, V.A., Negri, M. Pietro, Basso, D., 2023. The bryozoan margaretta cereoides as habitat-former in the coralligenous of marzamemi (SE Sicily, Mediterranean Sea). J Mar Sci Eng 11, 590. https://doi.org/10.3390/jmse11030590.
Sanfilippo, R., Rosso, A., Basso, D., Violanti, D., Di Geronimo, I., Di Geronimo, R., Benzoni, F., Robba, E., 2011. Cobbles colonization pattern from a tsunami-affected coastal area (SW Thailand, Andaman Sea). Facies 57, 1–13. https://doi.org/10.1007/S10347-010-0226-0/FIGURES/9.
Sanfilippo, R., Vertino, A., Rosso, A., Beuck, L., Freiwald, A., Taviani, M., 2013. Serpula aggregates and their role in deep-sea coral communities in the southern Adriatic Sea. Facies 59, 663–677. https://doi.org/10.1007/S10347-012-0356-7/FIGURES/8.
Sanfilippo, R., Donato, G., Reitano, A., Serio, D., Bracchi, V.A., Negri, M. Pietro, Basso, D., Rosso, A., 2024. Habit and behaviour of the nestling bivalve *Gregariella semigranata* (Reeve, 1858) from the Mediterranean Coralligenous, 66, 103–113. https://doi.org/10.4002/040.066.0104.
Sartoretto, S., 1998. Bioérosion des concrétions coralligènes de Méditerranée pal les organismes perforants: essai de quantification de processus. Comptes Rendus de l'Académie des Sciences-Series IIA-Earth and Planetary Science 327 (12), 839–844.
Sartoretto, S., Verlaque, M., Laborel, J., 1996. Age of settlement and accumulation rate of submarie "coralligène" (−10 to -60m) of the northwestern Mediterranean Sea; relation to Holocene rise in sea level. Mar. Geol. 130, 317–331.
Scicchitano, G., Antonioli, F., Berlinghieri, E.F.C., Dutton, A., Monaco, C., 2008. Submerged archaeological sites along the Ionian coast of southeastern Sicily (Italy) and implications for the Holocene relative sea-level change. Quat. Res. 70, 26–39. https://doi.org/10.1016/j.yqres.2008.03.008.
Teichert, S., 2014. Hollow rhodoliths increase Svalbard's shelf biodiversity. Sci. Rep. 4, 1–5. https://doi.org/10.1038/srep06972.
Teixidó, N., Garrabou, J., Harmelin, J.G., 2011. Low dynamics, high longevity and persistence of sessile structural species dwelling on mediterranean coralligenous outcrops. PLoS ONE 6, e23744. https://doi.org/10.1371/JOURNAL.PONE.0023744.
Torrano-Silva, B.N., Ferreira, S.G., Oliveira, M.C., 2015. Unveiling privacy: advances in microtomography of coralline algae. Micron 72, 34–38. https://doi.org/10.1016/J.MICRON.2015.02.004.
Varzi, A.G., Fallati, L., Savini, A., Bracchi, V.A., Bazzicalupo, P., Rosso, A., Sanfilippo, R., Bertolino, M., Muzzupappa, M., Basso, D., Giulia Varzi, A., 2023. Geomorphology of coralligenous reefs offshore southeastern Sicily (Ionian Sea). J. Maps 19, 1–13. https://doi.org/10.1080/17445647.2022.2161963.
Varzi, A.G., Meschis, M., Fallati, L., Scicchitano, G., De Santis, V., Scardino, G., Basso, D., Bracchi, V.A., Savini, A., 2024. New chronology for submerged relict paleoshorelines and associated rates of crustal vertical movements offshore the Marzamemi village, Sicily (Southern Italy). Mar. Geol. 474, 107326. https://doi.org/10.1016/J.MARGEO.2024.107326.
Walczak, I.W., Baldini, J.U.L., Baldini, L.M., McDermott, F., Marsden, S., Standish, C.D., Richards, D.A., Andreo, B., Slater, J., 2015. Reconstructing high-resolution climate using CT scanning of unsectioned stalagmites: a case study identifying the mid-Holocene onset of the Mediterranean climate in southern Iberia. Quat. Sci. Rev. 127, 117–128. https://doi.org/10.1016/J.QUASCIREV.2015.06.013.
Zhang, D.Z., Zhang, P.Z., Sang, W.C., Cheng, H., Wu, X.P., Yuan, Y., Bai, Y.J., Wang, J.L., Jia, J.H., 2010. Implications of stalagmite density for past climate change: an example from stalagmite growth during the last deglaciation from Wanxiang Cave, western Loess Plateau. Chin. Sci. Bull. 55, 3936–3943. https://doi.org/10.1007/S11434-010-4190-4/METRICS.